NR2B subunit of the NMDA glutamate receptor regulates appetite in the parabrachial nucleus

Qi Wu[a,b,c,d,1], Ruimao Zheng[e,1], Dollada Srisai[c,d], G. Stanley McKnight[e], and Richard D. Palmiter[a,b,2]

Departments of [a]Biochemistry and [e]Pharmacology and [b]Howard Hughes Medical Institute, University of Washington School of Medicine, Seattle, WA 98195; and [c]Department of Pharmacology and [d]Eagles Diabetes Research Center, Carver College of Medicine, University of Iowa, Iowa City, IA 52242

Contributed by Richard D. Palmiter, July 26, 2013 (sent for review June 16, 2013)

Diphtheria toxin-mediated, acute ablation of hypothalamic neurons expressing agouti-related protein (AgRP) in adult mice leads to anorexia and starvation within 7 d that is caused by hyperactivity of neurons within the parabrachial nucleus (PBN). Because NMDA glutamate receptors are involved in various synaptic plasticity-based behavioral modifications, we hypothesized that modulation of the NR2A and NR2B subunits of the NMDA receptor in PBN neurons could contribute to the anorexia phenotype. We observed by Western blot analyses that ablation of AgRP neurons results in enhanced expression of NR2B along with a modest suppression of NR2A. Interestingly, systemic administration of LiCl in a critical time window before AgRP neuron ablation abolished the anorectic response. LiCl treatment suppressed NR2B levels in the PBN and ameliorated the local Fos induction that is associated with anorexia. This protective role of LiCl on feeding was blunted in vagotomized mice. Chronic infusion of RO25-6981, a selective NR2B inhibitor, into the PBN recapitulated the role of LiCl in maintaining feeding after AgRP neuron ablation. We suggest that the accumulation of NR2B subunits in the PBN contributes to aphagia in response to AgRP neuron ablation and may be involved in other forms of anorexia.

feeding behavior | nausea | NR2B signaling

NMDA receptors form glutamate-gated ion channels that mediate many forms of synaptic plasticity under physiological conditions and neuronal death under excitotoxic pathological conditions (1, 2). NMDA receptors are tetrameric complexes composed of two obligatory NR1 subunits and two regulatory NR2 and/or NR3 subunits. Multiple subtypes of NMDA receptors are identified with distinct pharmacological and biophysical properties that are predominantly determined by the type of NR2 subunit (NR2A to NR2D). NR2A and NR2B subunits are the most abundant subunits in the adult brain and differ in channel properties, synaptic localization, and protein interaction elements, all of which can contribute to the induction of synaptic plasticity (3). Some recent studies suggest that NMDA receptors play a major role in regulating feeding behavior and energy homeostasis. For example, antagonism of hindbrain NMDA receptors increases food intake, whereas activation of NMDA receptors in the nucleus tractus solitarius (NTS) is necessary for cholecystokinin-induced reduction of food intake (4, 5). Injection of NMDA receptor agonists into the lateral hypothalamus elicits feeding in satiated animals, whereas NMDA blockade suppresses food intake and can reduce body weight (6). Genetic inactivation of NR1 subunits specifically in agouti-related protein (AgRP) neurons results in marked loss of food intake and body fat and impaired feeding after a fast (7). These findings implicate NMDA receptor signaling within several neuronal circuits in the control of feeding and energy balance.

Emerging evidence suggests that a complex neural network including GABAergic AgRP neurons in the hypothalamic arcuate nucleus plays a pivotal role in the control of appetite and energy metabolism (8–10). Activation of AgRP neurons promotes food intake and body weight gain by inhibiting postsynaptic target neurons in the paraventricular hypothalamus (10). Ablation of AgRP neurons by administration of diphtheria toxin (DT) to mice that express the diphtheria toxin receptor (DTR) selectively in AgRP neurons ($Agrp^{DTR}$ mice) results in aphagia and a fatal loss of body weight caused by the hyperactivity of postsynaptic neurons in the parabrachial nucleus (PBN) as a consequence of losing inhibitory GABAergic signals (11–13). This anorexic response can be prevented by benzodiazepine potentiation of GABA signaling, by genetic blockade of NMDA glutamate receptor signaling in the PBN, or by reducing glutamatergic input or output from the PBN, including knockdown of NMDA expression in the PBN (14). However, the physiological roles of NMDA receptors in the PBN in modulating appetitive behavior have not been identified.

We explored the potential benefit of pretreatment with LiCl because this salt has been shown to affect the activity of the PBN and to modulate NMDA receptor functions. Lithium is commonly used to treat bipolar mood disorder, but it also can elicit robust neuroprotection against excitotoxicity in CNS neurons (15, 16). Long-term exposure to LiCl protects cultured cerebellar, cortical, and hippocampal neurons against glutamate-induced excitotoxicity; this protection can be attributed, in part, to the inhibition of NMDA receptor-mediated calcium influx (17). Significant weight gain is associated with prolonged lithium therapy in patients with bipolar disorder; these patients have enhanced preference for a high-calorie diet, but the mechanism (s) causing this metabolic effect are unknown (18). It is well documented that a single i.p. dose of LiCl produces gastrointestinal malaise that is coincident with the induction of Fos in certain brainstem structures, including the NTS and the PBN

Significance

Nausea, which can be induced by injecting LiCl i.p. in rodents, activates a neural circuit (vagus → nucleus tractus solitarius → parabrachial nucleus) that promotes severe anorexia. Ablation of orexigenic neurons in the hypothalamus that express agouti-related protein (AgRP) also activates this anorexia pathway and leads to starvation. Here we show that pretreatment of mice with LiCl prevents starvation after ablation of AgRP-expressing neurons. The mechanism of protection involves suppression of the increase in the NR2B subunit of the NMDA receptor in the parabrachial nucleus that occurs after AgRP neuron ablation. We suggest that preactivation of the nausea circuit promotes synaptic changes that compensate for the loss of the input from AgRP-expressing neurons and thereby prevents starvation.

Author contributions: Q.W. and R.D.P. designed research; Q.W., R.Z., and D.S. performed research; Q.W., G.S.M., and R.D.P. contributed new reagents/analytic tools; Q.W., R.Z., and D.S. analyzed data; and Q.W. and R.D.P. wrote the paper.

The authors declare no conflict of interest.

Freely available online through the PNAS open access option.

[1]Q.W. and R.Z. contributed equally to this work.

[2]To whom correspondence should be addressed. E-mail: palmiter@uw.edu.

This article contains supporting information online at www.pnas.org/lookup/suppl/doi:10.1073/pnas.1314137110/-/DCSupplemental.

(19, 20). Exposure of rodents to a novel taste followed by LiCl treatment produces robust conditioned aversion to that taste, and electrolytic lesions of the PBN prevent LiCl-mediated conditioned taste aversion (21). These results are consistent with the idea that LiCl activates vagal afferents to the NTS, which then relays an excitatory, glutamatergic signal to the PBN where it induces Fos in a subpopulation of PBN neurons. We hypothesized that robust glutamatergic signaling induced in the PBN by LiCl treatment might lead to synaptic plasticity involving NMDA receptors and that these changes might influence the anorexia phenotype associated with the sudden loss of GABAergic input to the PBN from AgRP neurons.

Results

LiCl Pretreatment Prevents Severe Aphagia Caused by AgRP Neuron Ablation. Because prolonged activation of excitatory neurons leads to adaptive desensitization in certain types of hippocampal and cortex neurons (22–26), we hypothesized that recurrent treatment with LiCl might dampen the excitability of glutamatergic neurons in the PBN when GABAergic input from AgRP neurons is abolished and thereby protect against aphagia. To test this hypothesis, $Agrp^{DTR/+}$ and wild-type (C57BL/6) mice were treated i.p. with saline or LiCl (0.25 M, 10 $\mu L \cdot g^{-1} \cdot d^{-1}$) for four consecutive days. DT-mediated ablation of AgRP neurons was initiated 24 h after termination of the LiCl treatment. Daily administration of LiCl had little effect on food intake and body weight except for a small and transient loss of appetite after the first few injections. (Fig. 1). Remarkably, LiCl pretreatment prevented the severe aphagia and weight loss associated with DT treatment of $Agrp^{DTR/+}$ mice, whereas the mice treated with normal saline stopped eating by day 7 (Fig. 1). Treatment of wild-type mice with LiCl and DT had little effect on body weight, but food intake was reduced during the first few days.

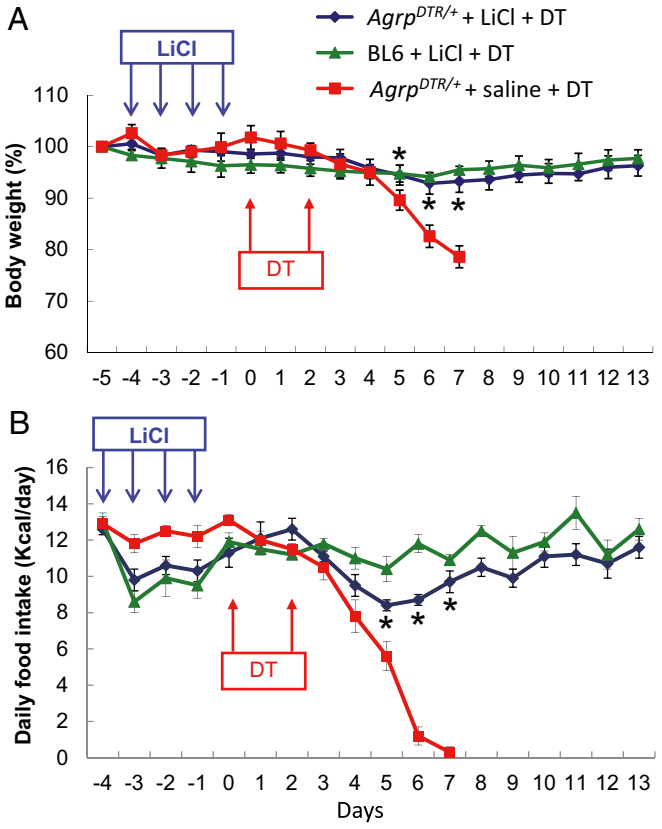

Fig. 1. Prolonged administration of LiCl prevents aphagia in AgRP neuron-ablated mice. (*A*) Body weight of $Agrp^{DTR/+}$ mice and wild-type (BL6) mice after 4 d of saline or LiCl treatment (0.25 M, 10 $\mu L \cdot g^{-1} \cdot d^{-1}$, i.p.; $n = 8$ per group). DT-mediated ablation of AgRP neurons was initiated 1 d after LiCl treatment was terminated, and DT was administered i.m. twice as indicated by arrows. (*B*) Daily food intake was measured for the groups of mice described in *A*. *$P < 0.05$ between $Agrp^{DTR/+}$ mice treated with LiCl and $Agrp^{DTR/+}$ mice treated with saline for both body weight and food intake; two-way, repeated-measures ANOVA. Results are shown as means ± SEM.

To understand better the conditions in which LiCl treatment was able to maintain feeding, we examined different time windows of LiCl treatment before ablation of AgRP neurons. In contrast to the previous experiment in which DT was given 1 d after LiCl treatment ceased, DT injection was initiated 2 or 3 d after the last of four daily LiCl treatments. We found that the efficacy of LiCl against starvation was still intact when ablation of AgRP neurons was initiated 2 d after termination of the LiCl treatment (Fig. 2). However, the protective effect of LiCl was abolished in the mice in which DT was administered 3 d after LiCl treatment (Fig. 2). These experiments demonstrate that the protective effect of LiCl treatment lasts for 2 d and then dissipates.

Pretreatment with LiCl Reduces Fos Induction in the PBN After Ablation of AgRP Neurons. LiCl treatment has been shown to induce neuronal excitability and subsequent adaptation in the hippocampal and cortical neurons (27–29). We therefore speculated that LiCl-mediated activation of PBN neurons might promote a reversible adaptation in the feeding circuitry to compensate for the sudden loss of inhibitory input from AgRP neurons. Loss of AgRP neurons results in Fos induction in the same region of the PBN where Fos induction occurs after a single injection of LiCl (Fig. 3 *A* and *B*), in agreement with previous results (13). However, the Fos signal in the PBN neurons was reduced dramatically in $Agrp^{DTR/+}$ mice to which LiCl had been administered previously for four consecutive days (Fig. 3*C*), and Fos was maintained at baseline level when AgRP neurons subsequently were killed by DT treatment (Fig. 3*D*). These results (quantified in Fig. 3*E*) suggest that PBN neurons adapt to repeated exposure to i.p. LiCl treatments so that they no longer are excited by loss of GABA signaling from AgRP neurons.

To ascertain whether LiCl exerts its effect on feeding through direct modulation of neuronal activity in the PBN, osmotic minipumps were used to infuse LiCl chronically either into the fourth ventricle or directly into the PBN before $Agrp^{DTR/+}$ mice were treated with DT. We found that central administration of LiCl by either route failed to protect against the starvation phenotype regardless of the dose (Fig. S1). Because LiCl promotes the formation of conditioned taste aversion and elevates Fos activity in the NTS and PBN by activating vagus nerves (30, 31), we examined the effect of gastric vagotomy on LiCl-induced protection. The protective role of LiCl on feeding and body weight of AgRP-ablated mice was abolished completely in vagotomized mice as compared with controls treated with sham surgery (Fig. S2). These results suggest that LiCl exerts its protective effect on the PBN by activating vagal afferents to the NTS which then are relayed to the PBN (14).

LiCl Pretreatment Prevents Changes in NMDA Receptor Subunit Abundance. Our previous experiments implicated glutamate signaling onto NMDA receptors of PBN neurons as the source of excitation that results in Fos induction and aphagia (14). We hypothesized that acute ablation of AgRP neurons, which could result in a homeostatic increase of PBN excitation, might trigger compensatory changes in the expression profile of the NR2A and NR2B subunits of the NMDA receptor. We measured both total and phosphorylated (activated) forms of NR2A and NR2B subunits from the PBN during the 6-d period after DT treatment of $Agrp^{DTR/+}$ mice by Western blot from tissue punches centered on the PBN. We chose antibodies against specific tyrosine residues

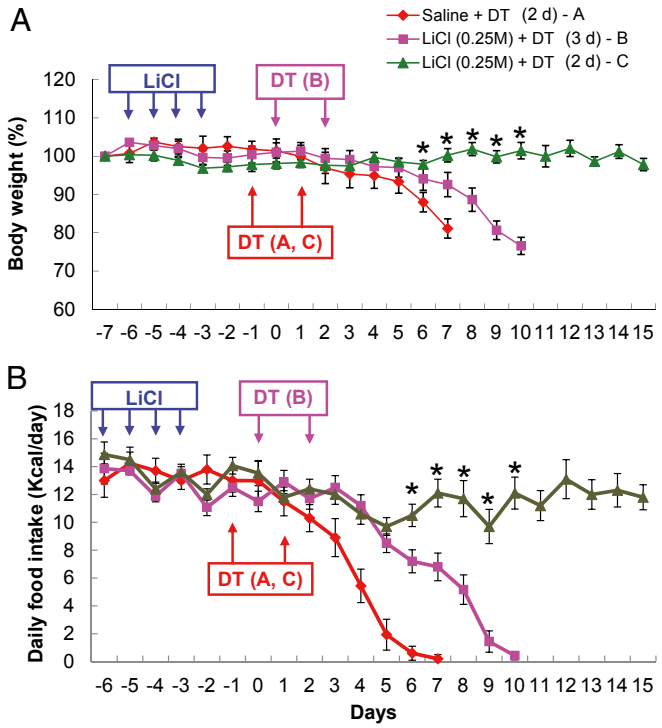

Fig. 2. The effect of LiCl treatment on restoration of appetite in AgRP neuron-ablated mice is transient. (*A*) Body weight of $Agrp^{DTR/+}$ mice after 4 d of saline or LiCl treatment (0.25 M, 10 μL·g^{-1}·d^{-1}, i.p.; n = 6–8 per group). Injection of DT was initiated either 2 d (red line A and green line C traces) or 3 d (purple line B trace) after LiCl treatment was terminated. (*B*) Daily food intake was measured for the groups of mice described in *A*. Two-way, repeated-measures ANOVA revealed (*i*) no effect of LiCl treatment on either body weight or food intake from day −7 to day 0; (*ii*) a significant effect on both body weight and food intake at days 1–7 in saline-treated and LiCl-treated groups with a 2-d delay before DT treatment (*$P < 0.05$); and (*iii*) a significant effect of LiCl on both body weight and food intake from days 1–10 after 2-d vs. 3-d delay in DT treatment (*$P < 0.05$). Results are shown as means ± SEM.

in NR2A [phosphorylated NR2A (pNR2A), Tyr1325] and NR2B [phosphorylated NR2B (pNR2B), Tyr1742] that are most relevant to synaptic modulation of neuronal excitability and neuroprotection (32, 33). The total NR2A and pNR2A in the PBN were largely insensitive to the ablation of AgRP neurons (Fig. 4*A*), whereas both total NR2B and pNR2B showed progressive elevation after $Agrp^{DTR/+}$ mice were treated with DT (Fig. 4*B*). Both NR2B and pNR2B reached their peak levels (approximately twofold higher than baseline) on the fifth day after DT treatment. Immunostaining results also indicated a significant increase in NR2B expression in the PBN 5 d after the ablation of AgRP neurons (Fig. S3). There were no changes in NR2B levels in the periaqueductal gray region of the brain, another target of AgRP neurons. These results suggest that NR2B signaling in the PBN is potentiated upon removal of GABAergic input from AgRP neurons and might promote anorexia. In a control experiment in which naive $Agrp^{DTR/+}$ mice and DT-treated $Agrp^{DTR/+}$ mice were pair-fed, the level of total NR2B and pNR2B in the PBN neurons remained unchanged (Fig. 4*D*). However, the total and pNR2A displayed a transient but significant reduction during the first 3 d in response to pair-feeding (Fig. 4*C*). This decrease in NR2A might reflect an adaptation to starvation.

To establish further the relationship between NMDA receptor signaling and appetitive behavior in the AgRP neuron-ablated mice, we examined the level of total NR2A and NR2B in the PBN after chronic infusion of bretazenil (a $GABA_A$ receptor agonist) into the PBN, a procedure that prevents severe aphagia and allows the mice to recover normal feeding (13). Western blot data revealed that chronic treatment with bretazenil modestly reduced NR2B expression compared with a group of mice treated with DT alone (Fig. 5). Four days of treatment with LiCl significantly reduced NR2B levels and modestly enhanced NR2A abundance compared with that in naive mice (Fig. 5). Furthermore, pretreatment with LiCl for 4 d completely prevented the enhanced expression of NR2B that occurs after DT-mediated ablation of AgRP neurons (Fig. 5). Immunostaining results indicated that the accumulation of NR2B subunits after ablation of AgRP neurons was colocalized to a large extent with Fos signals in PBN neurons (Fig. S3). Taken together with the previous time-course study, these results suggest that enhanced NR2B signaling in the PBN is tightly associated with the anorexic phenotype in this AgRP neuron-ablation model.

Pharmacological Suppression of NR2B Activity Protects Against Aphagia After AgRP Neuron Ablation. To determine the functional contribution of NR2B signaling in the PBN to appetitive behavior, a selective NR2B antagonist, RO25-6981, was infused bilaterally into the PBN via a 14-d osmotic minipump starting 5 d before the ablation of AgRP neurons (34). We observed a dose-dependent amelioration of the aphagia phenotype; the highest

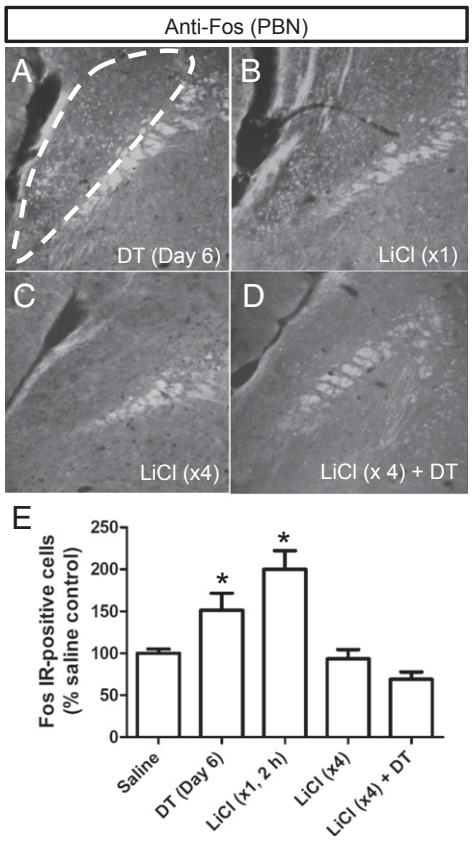

Fig. 3. Prolonged treatment with LiCl prevents Fos activation in the lateral PBN after ablation of AgRP neurons. (*A–D*) Representative immunohistochemistry images of Fos in neurons from the lateral PBN of $Agrp^{DTR/+}$ mice (*A*) 6 d after DT-mediated ablation of AgRP neurons; (*B*) 2 h after acute LiCl treatment; (*C*) 4 d after prolonged treatment of LiCl (tissues were collected 2 h after the last LiCl treatment); and (*D*) 4 d of LiCl treatment followed by DT administration (tissues were collected 6 d after the initiation of DT treatment). (*E*) Quantified immunoreactivity of Fos^+ neurons in the lateral PBN after each of the four treatments. *$P < 0.01$, (ANOVA); n = 6 mice per group. Results are shown as means ± SEM.

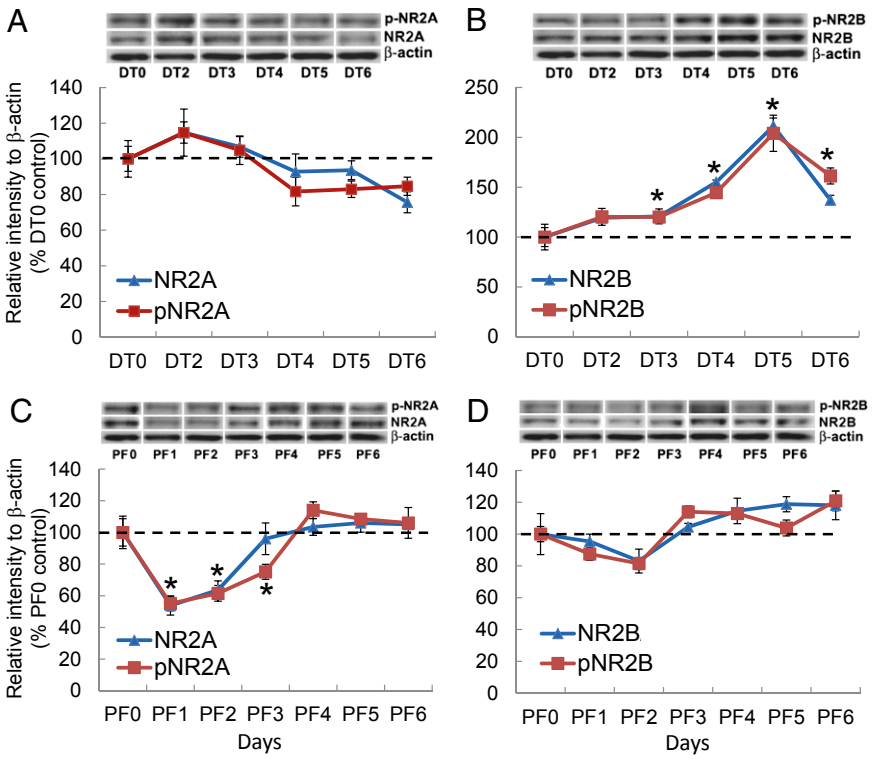

Fig. 4. The NR2B subunit is up-regulated in the PBN neurons after acute ablation of AgRP neurons. (*A* and *C*) Western blot analysis showing the progressive change in the relative abundance of total NR2A and pNR2A (Tyr1325) in the PBN of $Agrp^{DTR/+}$ mice after DT-mediated ablation of AgRP neurons (*A*) and after pair-feeding (PF) (*C*). (*B* and *D*) Western blot analysis showing the relative abundance of total NR2B and phosphorylated NR2B (Tyr1742) in the PBN of $Agrp^{DTR/+}$ mice after DT-mediated ablation of AgRP neurons (*B*) and after pair-feeding (PF) (*D*). *$P < 0.01$; ANOVA; $n = 5$ or 6 mice per group. In all Western blots, β-actin serves as the control. Results are shown as means ± SEM. DT0–DT6, days of DT treatment; PF0–PF6, days of pair-feeding matched to that consumed by the DT-treated group.

dose completely protected against aphagia and loss of body weight (Fig. 6). Interestingly, infusion of RO25-6981 into the PBN caused significant enhancement of daily food intake and body weight gain during the first 5 d of minipump treatment in naive $Agrp^{DTR/+}$ mice (Fig. 6). Moreover, the appetitive behavior was rescued completely in AgRP neuron-ablated mice when the NR2B antagonist and the $GABA_A$ receptor agonist were infused simultaneously into the PBN at doses that by themselves would maintain appetite only partially (Fig. 6). Coordinates for histological sites receiving NR2B antagonist and/or bretazenil infusion into the PBN are illustrated in Fig. S4. These results indicate that blockade of NR2B signaling in the PBN is sufficient to prevent anorexic response when AgRP neurons are ablated in adult mice.

Discussion

Our experiments reveal that pretreatment with LiCl prevented the hyperactivity of postsynaptic neurons in the PBN after acute ablation of inhibitory AgRP neurons, thereby maintaining normal food intake and body weight. The mechanism underlying the role of LiCl on the PBN was linked to NMDA receptor signaling. It has been suggested that chronic treatment of LiCl protects against excitotoxicity in cortical neurons by selective inhibition of tyrosine phosphorylation in the NMDA receptor NR2B subunits (33). However, we observed a significant reduction of total NR2B in the PBN when LiCl was administered systemically. Consistent with the findings that prolonged activation of excitatory neurons leads to adaptive desensitization, our data suggest that peripheral administration of LiCl, by acting through vagal afferents, modulates total NR2B expression within PBN neurons, in turn leading to the suppression of neuronal excitability. Preventing excessive signaling by NR2B-containing NMDA receptors, either by preventing their accumulation or by inhibiting their activity with an antagonist, protects against the hyperactivity and aphagia that otherwise would ensue following ablation of AgRP neurons.

The neurons in the PBN that become Fos^+ after treatment with LiCl or after ablation of AgRP neurons reside in the external lateral region of the PBN. This region includes neurons that express calcitonin gene-related protein (CGRP) and project to the lateral capsule of the amygdala. Photoactivation of those neurons with channel rhodopsin or pharmacological activation of the HM3q DREADD receptor in those neurons is sufficient to inhibit food intake in a transient or tonic manner, respectively (35). We anticipate that the NR2B subunits accumulate primarily in the CGRP neurons in the external lateral region of the PBN because we observe accumulation of NR2B in Fos^+ neurons in that brain region. Future studies need to examine the extent of NMDA receptor changes in CGRP-expressing neurons by cell-specific biochemical and electrophysiological methods.

The accumulation of NR2B subunits after the loss of AgRP neurons seems maladaptive, because we would expect homeostatic mechanisms to be engaged that would reduce neuronal excitability after loss of GABA signaling from AgRP neurons. Perhaps the induction of NR2B is not an adaptive mechanism but rather is a response to the degeneration of AgRP neuron axon terminals. We showed previously that both microglia and astrocytes are activated in postsynaptic target regions after ablation of AgRP neurons (12). Those activated glial cells release cytokines (such as IL-1β, TNF-α, and IL-6) that affect the expression of NMDA receptor subunits in other systems (36–38). We have shown that mice eventually adapt to the loss of AgRP neurons, but the adaptation process takes about 10 d, during which time glial activation may subside. In this scenario, intervention

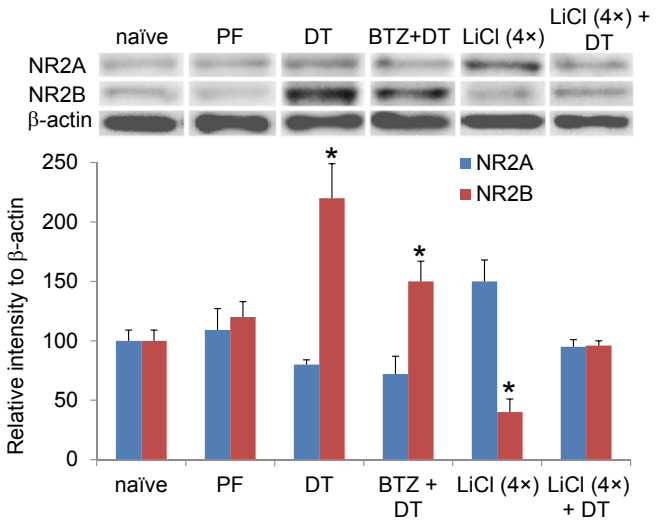

Fig. 5. The abundance NR2B in the PBN is attenuated after chronic administration of bretazenil or prolonged treatment with LiCl. Western blot analysis showed the relative abundance of total NR2A and NR2B in the PBN neurons of naive *Agrp*$^{DTR/+}$ mice (naive); pair-fed naive mice (PF) and DT-treated *Agrp*$^{DTR/+}$ mice (DT); DT-treated *Agrp*$^{DTR/+}$ mice treated with chronic infusion of bretazenil (0.3 mg/mL) into the fourth ventricle (BTZ + DT); *Agrp*$^{DTR/+}$ mice with prolonged treatment of LiCl [LiCl (4×)]; and *Agrp*$^{DTR/+}$ mice with prolonged treatment of LiCl followed by DT [LiCl (4×) + DT]. β-Actin served as the control. *$P < 0.01$, ANOVA; $n = 6$–10 mice per group. Results are shown as means ± SEM. Tissue was collected 5 d after initiation of treatment for PF, DT, LiCl (4×) groups; 10 d after initiation of treatment for LiCl (4×)+DT group (5 d after DT); and 14 d after initiation of treatment for BTZ+DT group, i.e. when feeding had been restored.

either by pretreatment with LiCl or by administering the NR2B antagonist during the ablation period prevents the induction of the maladaptive phenotype that is induced by loss of AgRP axon terminals in the PBN.

Methods

Mice. Male mice were housed in a temperature- and humidity-controlled facility with a 12-h light/dark cycle. All animal care and experimental procedures were approved by the Institutional Animal Care and Use Committee at the University of Washington and the University of Iowa. In compliance with our approved protocol, all experiments were terminated if the body weight of mice fell to 80% of their original body weight. *Agrp*$^{DTR/+}$ mice were generated by targeting the human diphtheria toxin receptor (heparin-binding epidermal growth factor) to the *Agrp* locus (11). Mice were group housed with standard chow diet (Lab-Diet 5053) and water provided ad libitum until the beginning of the experiments.

Subdiaphragmatic Gastric Vagotomy. The mice were deeply anesthetized by i.p. injection of ketamine and xylazine. After s.c. injection of buprenorphine, a 12-mm midline incision was made posterior to the xiphisternum; the left and right vagus nerves were located on the lateral border of the abdominal esophagus and were separated from the surrounding peritoneal tissue, and gastric nerve trunks (~10 mm long) were cut under a dissecting microscope. The abdominal wall and skin were closed with sterile nylon suture; the skin suture was removed 10 d after the surgery. Subdiaphragmatic gastric vagotomy results in dilated gastric ventricles, which were obvious in vagotomized mice but not in sham-operated mice.

Food Intake and Body Weight Measurements. For feeding assays, mice were transferred to BioDAQ Food and Water Intake Monitor (Research Diets) and were supplied with water and low-fat (3.85 kcal/mL) chow diet (D12450B; Research Diets). The mice were allowed to acclimate for 3 d before the initiation of each experiment and data collection. Body weight and total food intake were recorded every 24 h. Feeding and drinking activity was recorded in accordance with the manufacturer's suggested protocol.

Pharmacological Treatments. To ablate AgRP neurons in adult mice, we administered two i.m. injections of DT (50 mg/kg; List Biological Laboratories) 2 d apart to 6-wk-old mice (11). For systemic treatment, LiCl (0.25 M, 10 μL·g^{-1}·d^{-1}; Sigma-Aldrich) was dissolved in distilled water before i.p. injection. For central administration, Alzet 14-d minipumps (model 1002; Durect) loaded with 100 μL of LiCl, RO25-6981 (Sigma-Aldrich), or a mixture of RO25-6981 and bretazenil (Sigma-Aldrich) were implanted s.c. on the back of anesthetized mice 4 d before DT treatment. Surgical procedures of cannulation into fourth ventricle or bilaterally into the PBN followed published protocols (13). The patency and placement of the bilateral minipump were verified at the end of each experiment when brain samples were processed for immunohistological analysis.

Immunohistochemistry. On day 6 after DT injection, deeply anesthetized animals were perfused intracardially by ice-cold PBS followed by 4% (wt/vol) paraformaldehyde. Whole brain was dissected out and fixed overnight in 4% (wt/vol) paraformaldehyde before being moved to 30% sucrose where it was maintained until it sank. Then 25-μm frozen sections were cut by cryostat. The sections were incubated in 0.3% H_2O_2 for 20 min and then were washed twice with TBS-0.05% Tween 20 (TBST). The sections were incubated for 30 min in blocking buffer containing 0.1 M Tris·HCL (pH7.5), 0.15 M NaCl with 0.5% blocking reagent from the Cy3 Tyramide signal amplification system (PerkinElmer) according to the manufacturer's protocol. Rabbit anti-NR2B antibody (EMD Millipore) was diluted at 1:500 in blocking buffer, and sections were incubated in this antibody overnight at 4 °C. The sections were washed three times in TBST at room temperature and were incubated in HRP-conjugated donkey anti-rabbit IgG for 40 min. The sections were washed three times with TBST and incubated in fluorophore tyramide for 3 min at room temperature before being washed three times again in TBST. Before

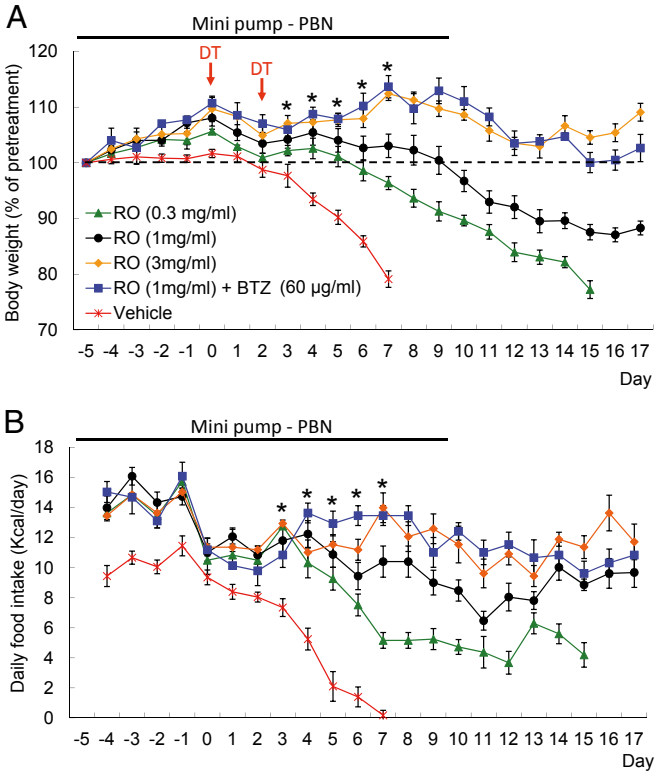

Fig. 6. Chronic administration of the NR2B subtype-selective antagonist RO25-6981 (RO) into the PBN area prevents aphagia in AgRP neuron-ablated mice. (*A*) Body weight of *Agrp*$^{DTR/+}$ mice after chronic infusion of RO25-6981 or vehicle bilaterally into the PBN ($n = 14$ per group). DT-mediated ablation of AgRP neurons was initiated 6 d after implantation of minipumps loaded with various doses of RO25-6981 and/or bretazenil (BTZ). (*B*) Daily food intake was measured for the groups of mice described in *A*. *$P < 0.01$; two-way, repeated-measures ANOVA between each of the RO25-6981-treated groups and the vehicle-treated group during days 3–7; $n = 6$–8 mice per group. Results are shown as means ± SEM.

treatment with the Fos antibody, the sections were incubated in 25 mM glycine, 10% (wt/vol) SDS, pH 2 for 30 min at 50 °C to elute the primary NR2B antibody. The sections were washed by TBS twice before being incubated in blocking solution [4% (vol/vol) normal donkey serum in TBST] for 1 h on a shaker. The sections were incubated in the primary antibody, anti-Fos antibody (PC38, EMD Millipore) at a dilution of 1:1,000 in blocking solution at 4 °C overnight. The sections were washed three times with TBST before being incubated in the secondary antibody, 1:400 Alexa Fluor 488-conjugated donkey anti-rabbit IgG (Jackson ImmunoResearch) for 30 min at room temperature. The sections were washed five times with TBST and were mounted on glass slides and covered with anti-fade mounting medium. Sections incubated without a primary antibody were used as negative control.

Western Blot Analysis. Tissue micropunches of 1-mm diameter (Fine Science Tools GmbH) including the PBN (39) were obtained bilaterally from 1-mm-thick coronal sections using a stainless steel mouse brain matrix (Harvard Apparatus), were rapidly frozen in liquid nitrogen, and were kept at −80 °C until further processing. Coordinates of collected brain regions were based on the Paxinos Mouse Brain Atlas (40). Samples were homogenized and sonicated separately in ice-cold RIPA buffer (41) supplemented with protease inhibitors (P8340; Sigma) and phosphatase inhibitor mixture-3 (P0044; Sigma) and then were cleared by centrifugation (4 °C, 10,000 × *g*; 20 min). Protein quantification was performed with the BCA assay kit (Thermo Scientific, Pierce). Protein samples (5 μg) of each brain region in SDS loading buffer were electrophoresed on 8% (wt/vol) SDS/PAGE gel and transferred to nitrocellulose membrane (Schleicher & Schuell). Membranes were blocked with 5% (wt/vol) BSA in TBST for 2 h at room temperature and then were incubated overnight at 4 °C with primary antibodies. The primary antibodies and dilutions were anti-NR2B, 1:500 (610417; BD Transduction Laboratories); anti-NR2A, 1:1,000 (612286; BD Transduction Laboratories); anti–phospho-NR2A, 1:1,000 (ab16646; Abcam); anti–phospho-NR2B, 1:1,000 (M2442; Sigma); and anti–β-actin antibody, 1:5,000 (Sigma; A5316). Then the blots were washed at least five times in TBST for 5 min each washing at room temperature. HRP-conjugated secondary antibody (Jackson ImmunoResearch) was applied at a 1:10,000 dilution in TBST plus 5% (wt/vol) BSA and was incubated for 2 h at room temperature. After the blots were washed five times for 5 min each washing, they were developed with an ECL assay kit (SuperSignal West Pico Chemiluminescent Substrate, 34087 or SuperSignal West Dura Extended Duration Substrate, 34076; Thermo Scientific, Pierce) and were analyzed with a Kodak Digital Imaging System. Protein levels were expressed as ratios of the signal densities, and β-actin was used as a control for variations in protein loading.

Statistical Analyses. Quantification of Fos^+ cells was done using the NIH Image software (National Institutes of Health). From the anatomically matched sections of controls, a region of interest of the same size was defined. Meanwhile, an optimized threshold that can distinguish round Fos^+ nuclei from partially stained ones and from background noise was preset for all measurements. The total number of pixels of Fos^+ cells inside the defined region was recorded automatically. Unless otherwise stated, datasets collected from all experiments were analyzed by two-way, repeated-measures ANOVA followed by the Student–Newman–Keuls method for statistical significance and plotted as means ± SEM. Post hoc analysis was performed when group differences were significant by ANOVA at $P < 0.05$.

ACKNOWLEDGMENTS. We thank Drs. Matt Carter, Carolyn Roman, and Victor Derkach for constructive comments during the execution of these experiments and in the preparation of the manuscript and Dr. Yin Liu for help with quantitative analysis of Western blot data. This work was supported in part by National Institutes of Health Grants R01DA24908 and R01GM032875.

1. Paoletti P, Neyton J (2007) NMDA receptor subunits: Function and pharmacology. *Curr Opin Pharmacol* 7(1):39–47.
2. Traynelis SF, et al. (2010) Glutamate receptor ion channels: Structure, regulation, and function. *Pharmacol Rev* 62(3):405–496.
3. Yashiro K, Philpot BD (2008) Regulation of NMDA receptor subunit expression and its implications for LTD, LTP, and metaplasticity. *Neuropharmacology* 55(7):1081–1094.
4. Hung CY, Covasa M, Ritter RC, Burns GA (2006) Hindbrain administration of NMDA receptor antagonist AP-5 increases food intake in the rat. *Am J Physiol Regul Integr Comp Physiol* 290(3):R642–R651.
5. Burns GA, Ritter RC (1997) The non-competitive NMDA antagonist MK-801 increases food intake in rats. *Pharmacol Biochem Behav* 56(1):145–149.
6. Stanley BG, Urstadt KR, Charles JR, Kee T (2011) Glutamate and GABA in lateral hypothalamic mechanisms controlling food intake. *Physiol Behav* 104(1):40–46.
7. Liu T, et al. (2012) Fasting activation of AgRP neurons requires NMDA receptors and involves spinogenesis and increased excitatory tone. *Neuron* 73(3):511–522.
8. Wu Q, Palmiter RD (2011) GABAergic signaling by AgRP neurons prevents anorexia via a melanocortin-independent mechanism. *Eur J Pharmacol* 660(1):21–27.
9. Morton GJ, Cummings DE, Baskin DG, Barsh GS, Schwartz MW (2006) Central nervous system control of food intake and body weight. *Nature* 443(7109):289–295.
10. Sternson SM (2013) Hypothalamic survival circuits: Blueprints for purposive behaviors. *Neuron* 77(5):810–824.
11. Luquet S, Perez FA, Hnasko TS, Palmiter RD (2005) NPY/AgRP neurons are essential for feeding in adult mice but can be ablated in neonates. *Science* 310(5748):683–685.
12. Wu Q, Howell MP, Palmiter RD (2008) Ablation of neurons expressing agouti-related protein activates fos and gliosis in postsynaptic target regions. *J Neurosci* 28(37):9218–9226.
13. Wu Q, Boyle MP, Palmiter RD (2009) Loss of GABAergic signaling by AgRP neurons to the parabrachial nucleus leads to starvation. *Cell* 137(7):1225–1234.
14. Wu Q, Clark MS, Palmiter RD (2012) Deciphering a neuronal circuit that mediates appetite. *Nature* 483(7391):594–597.
15. Chuang DM (2005) The antiapoptotic actions of mood stabilizers: Molecular mechanisms and therapeutic potentials. *Ann N Y Acad Sci* 1053:195–204.
16. Schloesser RJ, Huang J, Klein PS, Manji HK (2008) Cellular plasticity cascades in the pathophysiology and treatment of bipolar disorder. *Neuropsychopharmacology* 33(1):110–133.
17. Nonaka S, Hough CJ, Chuang DM (1998) Chronic lithium treatment robustly protects neurons in the central nervous system against excitotoxicity by inhibiting N-methyl-D-aspartate receptor-mediated calcium influx. *Proc Natl Acad Sci USA* 95(5):2642–2647.
18. Livingstone C, Rampes H (2006) Lithium: A review of its metabolic adverse effects. *J Psychopharmacol* 20(3):347–355.
19. Lamprecht R, Dudai Y (1995) Differential modulation of brain immediate early genes by intraperitoneal LiCl. *Neuroreport* 7(1):289–293.
20. Swank MW, Bernstein IL (1994) c-Fos induction in response to a conditioned stimulus after single trial taste aversion learning. *Brain Res* 636(2):202–208.
21. Spector AC, Norgren R, Grill HJ (1992) Parabrachial gustatory lesions impair taste aversion learning in rats. *Behav Neurosci* 106(1):147–161.
22. Goel A, Buonomano DV (2013) Chronic electrical stimulation homeostatically decreases spontaneous activity, but paradoxically increases evoked network activity. *J Neurophysiol* 109(7):1824–1836.
23. Goold CP, Nicoll RA (2010) Single-cell optogenetic excitation drives homeostatic synaptic depression. *Neuron* 68(3):512–528.
24. Abraham WC, Bear MF (1996) Metaplasticity: The plasticity of synaptic plasticity. *Trends Neurosci* 19(4):126–130.
25. Turrigiano G (2012) Homeostatic synaptic plasticity: Local and global mechanisms for stabilizing neuronal function. *Cold Spring Harb Perspect Biol* 4(1):a005736.
26. Zorumski CF, Izumi Y (2012) NMDA receptors and metaplasticity: Mechanisms and possible roles in neuropsychiatric disorders. *Neurosci Biobehav Rev* 36(3):989–1000.
27. Yasoshima Y, Yamamoto T (1998) Short-term and long-term excitability changes of the insular cortical neurons after the acquisition of taste aversion learning in behaving rats. *Neuroscience* 84(1):1–5.
28. Lacaille JC, Cloutier S, Reader TA (1992) Lithium reduced synaptic transmission and increased neuronal excitability without altering endogenous serotonin, norepinephrine and dopamine in rat hippocampal slices in vitro. *Prog Neuropsychopharmacol Biol Psychiatry* 16(3):397–412.
29. Butler-Munro C, Coddington EJ, Shirley CH, Heyward PM (2010) Lithium modulates cortical excitability in vitro. *Brain Res* 1352:50–60.
30. Niijima A, Yamamoto T (1994) The effects of lithium chloride on the activity of the afferent nerve fibers from the abdominal visceral organs in the rat. *Brain Res Bull* 35(2):141–145.
31. Yamamoto T, et al. (1992) C-fos expression in the rat brain after intraperitoneal injection of lithium chloride. *Neuroreport* 3(12):1049–1052.
32. Taniguchi S, et al. (2009) Involvement of NMDAR2A tyrosine phosphorylation in depression-related behaviour. *EMBO J* 28(23):3717–3729.
33. Hashimoto R, Hough C, Nakazawa T, Yamamoto T, Chuang DM (2002) Lithium protection against glutamate excitotoxicity in rat cerebral cortical neurons: Involvement of NMDA receptor inhibition possibly by decreasing NR2B tyrosine phosphorylation. *J Neurochem* 80(4):589–597.
34. Liu Y, et al. (2007) NMDA receptor subunits have differential roles in mediating excitotoxic neuronal death both in vitro and in vivo. *J Neurosci* 27(11):2846–2857.
35. Carter ME, Soden ME, Zweifel LS, Palmiter RD (2013) Genetic identification of a neural circuit that suppresses appetite. *Nature*, in press.
36. Rai S, Kamat PK, Nath C, Shukla R (2013) A study on neuroinflammation and NMDA receptor function in STZ (ICV) induced memory impaired rats. *J Neuroimmunol* 254(1-2):1–9.
37. Jing T, et al. (2010) Soluble factors from IL-1β-stimulated astrocytes activate NR1a/NR2B receptors: Implications for HIV-1-induced neurodegeneration. *Biochem Biophys Res Commun* 402(2):241–246.
38. Lundborg C, Westerlund A, Björklund U, Biber B, Hansson E (2011) Ifenprodil restores GDNF-evoked Ca(2+) signalling and Na(+)/K(+) -ATPase expression in inflammation-pretreated astrocytes. *J Neurochem* 119(4):686–696.
39. Palkovits M (1973) Isolated removal of hypothalamic or other brain nuclei of the rat. *Brain Res* 59:449–450.
40. Paxinos G, Franklin KBJ (2004) *The Mouse Brain in Stereotaxic Coordinates* (Elsevier Academic, Amsterdam), Compact 2nd Ed.
41. Yin X, Feng X, Takei Y, Hirokawa N (2012) Regulation of NMDA receptor transport: A KIF17-cargo binding/releasing underlies synaptic plasticity and memory in vivo. *J Neurosci* 32(16):5486–5499.